Central European Journal of Energetic Materials, **2015**, *12*(2), 271-286
ISSN 1733-7178
e-ISSN 2353-1843

Phase Diagrams of the MeNQ/HN and HN/NQ Binary Systems

Man-Man TIAN [1, 2], Hua-Rong LI [2], Ling CHEN [2], Xin JU [1, *], Yuan-Jie SHU [2,**]

[1]*Department of Physics, University of Science and Technology Beijing, Beijing, China*
[2]*Institute of Chemical Materials, China Academy of Engineering Physics, Mianyang, China*
*E-mails: * jux@ustb.edu.cn, ** syjfree@sohu.com*

Abstract: An equation for a binary phase diagram with two eutectic points was deduced from the Van't Hoff equation. The melting points of hydrazinium nitrate/nitroguanidine (HN/NQ) samples with different ratios, ranging from 0 to 1 mole fraction, were explored by differential scanning calorimetry (DSC). The results revealed the presence of two eutectic points in the phase diagram of the HN/NQ binary system. The dependence of temperature on the composition (T-X phase diagram) of HN/NQ was depicted based on the equation described by the DSC data. The phase diagram of MeNQ/HN, with only one eutectic point was constructed by substituting experimental data of the compositions and their corresponding temperatures into the Van't Hoff equation. The phase diagram with two or more eutectic points indicated the formation of new stable compounds with appropriate ratios of the two components; no new substance appeared in the system with only one eutectic point. Thus, the HN/NQ binary system showed the presence of a new substance, which is probably the HN/NQ co-crystal. No new substance was detected in the MeNQ/HN binary system. The results of the X-ray diffraction patterns agree with the findings from the phase diagrams.

Keywords: phase diagram, binary system, eutectic, DSC, XRD

1 Introduction

MeNQ (N-Methyl-N'-nitroguanidine)-based eutectic mixtures of energetic materials have been reported in many studies [1, 2]. It has been considered as

a material with the highest potential to replace TNT as the liquid carrier in cast explosives [3, 4]. NQ (Nitroguanidine) is usually used as a component in mixed explosives and propellants [5]. It has two crystal structures, namely α and β, the former being more stable than the latter. The crystals are white needles that are neither hygroscopic nor volatilize at room temperature [5, 6]. HN (Hydrazinium nitrate) can increase the explosive power of mixed explosives [7, 8], and has a melting point of approximately 70 °C. Adding HN to mixed explosives reduces the melting point of the mixture [9-11].

Many methods can be used to construct phase diagrams [12-16]. For example, the T-X phase diagram is based on the Van't Hoff equation, and the H-X phase diagram is based on the mixture law. The construction of an H-X phase diagram is quicker and simpler than that of a T-X phase diagram [17, 18]. However, an H-X phase diagram cannot be used to determine the composition of a mixture or its melting temperature. In addition, the mixture law at the present time has proved to be insufficiently exact [19].

A T-X phase diagram describes the relationship between the composition and the melting temperature. Theories and experiments concerning T-X phase diagrams have been studied in several articles [20-24]. Some binary T-X and H-X phase diagrams of energetic materials, such as those of Tetryl/PETN, PETN/RDX and RDX/NQ, have been constructed [25]. Based on binary phase diagram theory, previous studies obtained equations for ternary phase diagrams and constructed ternary phase diagrams using binary system data [26, 27]. Ying Hui Shao *et al*. [27] constructed ternary phase diagrams of some volatile energetic materials, including TNT/TNAZ/DNTF and TNAZ/DNTF/RDX, by high-pressure differential scanning calorimetry (DSC). Chapman [28] deduced the phase diagram of a binary system from the Van't Hoff equation and calculated the intermolecular interactions of common energetic materials. The results of these two methods were consistent.

The studies reported thus far focus on phase diagrams with only one eutectic point. However, some systems, such as the MeNQ/AN (Ammonium nitrate) system, have two eutectic points [1]. The study of the theory of phase diagrams with two eutectic points and the construction of the relevant diagrams for binary or ternary systems are important topics. Therefore, the present study aims to deduce a theory for a binary phase diagram with two eutectic points on the basis of the conditions of chemical equilibrium. A binary phase diagram of HN/NQ with two eutectic points was constructed using this theory and experimental DSC data. This study also revised some results on the MeNQ/HN binary system previously reported by our group [10].

2 Experimental

2.1 Materials

HN was prepared by neutralizing hydrazine hydrate with nitric acid. NQ (purity > 99.5%) was provided by the Institute of Chemical Materials of China Academy of Engineering Physics, and MeNQ was purchased from Tianjin. The HN/NQ and MeNQ/HN samples used in this study were produced by heating mixtures of HN and NQ (or MeNQ and HN) with specific mole fractions. The numerical order of samples with different mole fractions is shown in Table 1.

Table 1. Compositions and melting temperatures of the binary systems

HN/NQ				MeNQ/HN			
No.	NQ [mol fraction]	M.p. 1 [°C]	M.p. 2 [°C]	No.	MeNQ [mol fraction]	M.p. 1 [°C]	M.p. 2 [°C]
1	0	---	70.24	1	0.1	---	70.15
2	0.1	---	59.51	2	0.2	69.08	---
3	0.2	---	---	3	0.3	69.17	---
4	0.3	---	54.11	4	0.4	70.18	---
5	0.4	54.03	132.22	5	0.5	68.7	112.9
6	0.5	51.87	173.55	6	0.6	67.06	118.71
7	0.6	52.91	206.06	7	0.7	67.82	128.6
8	0.7	52.25	211.22	8	0.8	67.11	138.07
9	0.8	141.8	207.41	9	0.33	69.73	---
10	0.9	143.66	190.72	10	0.25	69.61	---
11	1	---	232	11	0.67	67.09	125.61
				12	0.75	67.18	132.57

2.2 Experimental methods

The binary phase diagrams and crystal structures of the samples were studied. To construct the phase diagrams, the melting points of the samples were obtained by DSC (Diamond DSC, Perkin Elmer). X-ray powder diffractometry (XRD, D8 Advance, BrukerAxs, Germany) was used to characterize the crystal structures of the pure substances and of the mixtures.

DSC: Approximately 2 mg of the sample was placed in an aluminum pan with an aluminum lid covering it. The system temperature ranged from 45 to 260 °C at a constant heating rate of 10 °C·min^{-1}, and measurements were performed under a 0.1 MPa dynamic nitrogen atmosphere.

XRD: Samples were ground to a fine powder, dusted onto a metallic shallow groove and a glass slide was placed over the groove to flatten the powder surface. The scanning range was $2\theta = 10\text{-}60°$.

3 Principle of the Phase Diagram of the Binary System

For a binary system of components A and B:

$$\frac{\mathrm{d}X^{\mathrm{sol}}}{\mathrm{d}T} - \frac{\mathrm{d}X^{\mathrm{liq}}}{\mathrm{d}T} = \frac{\Delta S_{\mathrm{A}}^{*}}{RT_{0\mathrm{A}}} = \frac{\Delta H_{\mathrm{A}}^{*}}{RT_{0\mathrm{A}}^{2}} \tag{1}$$

The solidus curve in the *T-X* phase diagram falls practically on the vertical (temperature) axis,

$$\frac{\mathrm{d}X^{\mathrm{sol}}}{\mathrm{d}T} = 0$$

Equation (1) can be written as:

$$\frac{\mathrm{d}X^{\mathrm{liq}}}{\mathrm{d}T} = -\frac{\Delta S_{i}^{*}}{RT_{0i}} = -\frac{\Delta H_{i}^{*}}{RT_{0i}^{2}} \tag{2}$$

where: X^{sol} and X^{liq} are the equilibrium mole fractions of the second component in the solid phase and the liquid phase, respectively, ΔS_i^* and ΔH_i^* are the entropy and the enthalpy of melting of the pure component i, and T_{0i} is the melting point of the pure component i, i = A, B, C.

For an isobaric binary system, the molar Gibbs energy of a mixed phase is given by:

$$G(T,X) = (1-X)\,\mu_{\mathrm{A}}(T,X) + X\,\mu_{\mathrm{B}}(T,X) \tag{3}$$

The thermodynamic potentials (= partial molar Gibbs energies) for the first and the second component in the homogeneous mixture are:

$$\mu_{\mathrm{A}}(T,X) = \mu_{\mathrm{A}}^{*}(T) + RT\ln(1-X) + \mu_{\mathrm{A}}^{\mathrm{E}}(T,X) \tag{4}$$

$$\mu_{\mathrm{B}}(T,X) = \mu_{\mathrm{B}}^{*}(T) + RT\ln X + \mu_{\mathrm{B}}^{\mathrm{E}}(T,X) \tag{5}$$

where: X is the mole fraction of component B, μ_i^* is the thermodynamic potential (= partial molar Gibbs energy) of the pure component i, μ_i^{E} stands for the molar excess thermodynamic potential, which is part of the thermodynamic potential that accounts for non-ideal mixing, i = A, B, C.

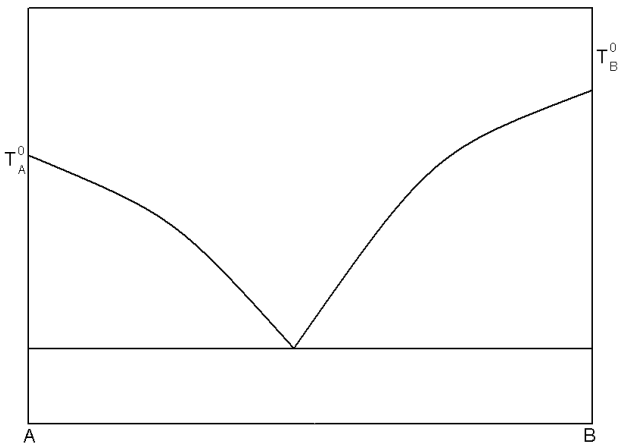

Figure 1. T-X phase diagram of a binary system with one eutectic point.

For a binary phase diagram (Figure 1) with only one eutectic point, the condition for the solid-liquid equilibrium between the solid pure component A and a liquid mixture with composition X can be written as:

$$\mu_A^{*\,sol}(T) = \mu_A^{liq}(T, X_e^{liq}) = \mu_A^{*\,liq}(T) + RT\ln(1-X_e^{liq}) + \mu_A^{E\,liq}(T,X_e^{liq}) \quad (6)$$

$$\mu_A^{*\,liq}(T) - \mu_A^{*\,sol}(T) = -RT\ln(1-X_e^{liq}) - \mu_A^{E\,liq}(T,X_e^{liq})$$
$$-\Delta S_A^*\,(T - T_{0A}) = -RT\ln(1-X_e^{liq}) - \mu_A^{E\,liq}(T,X_e^{liq}) \quad (7)$$

With:

$$\Delta S_A^* = \Delta H_A^* / T_{0A} \quad (8)$$

the expression of the liquid curve can be written as:

$$\ln(1-X) = \frac{\Delta H_A^*}{R}\left(\frac{1}{T_{0A}} - \frac{1}{T}\right) - \frac{\mu_A^E(T,X)}{RT} \quad (9)$$

When $X = 1$, $T = T_{0A,}$ it can be calculated that:

$$\mu_A^E = 0$$

Under this condition, Equation (9) is the same as the Van't Hoff equation [29, 30].

For a binary system in which a new compound $C(A_mB_n)$ is formed the chemical equation can be given as:

$C - mA - nB = 0$

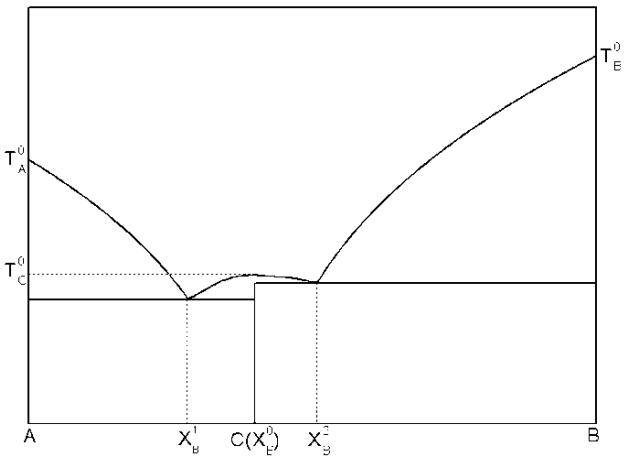

Figure 2. T-X phase diagram of a binary system with two eutectic points.

In the phase diagram (Figure 2) of this system, there are two eutectic points. The conditions for the chemical equilibrium between the solid pure component C and a liquid mixture is:

$$\mu_C^{*sol}(T) - m\mu_A^{liq}(T, X_e^{liq}) - n\mu_C^{liq}(T, X_e^{liq}) = 0 \tag{10}$$

$$\mu_C^{*sol}(T) - m[\mu_A^{*}(T) + RT\ln(1-X) + \mu_A^{E}(T,X)] - n(\mu_B^{*}(T) + RT\ln X + \mu_B^{E}(T,X)] = 0$$

$$\mu_C^{*sol}(T) - m\mu_A^{*}(T) - n\mu_B^{*}(T) = mRT\ln(1-X) + m\mu_A^{E}(T,X) + n\,RT\ln X + n\mu_B^{E}(T,X)$$

Making $\mu^E = (m\mu_A^E(T,X) + n\mu_B^E(T,X)]/\,RT,$

$$\Delta S_C^{*}\,(T - T_{0C}) = mRT\ln(1-X) + n\,RT\ln X + \mu^E\,RT \tag{11}$$

With:

$$\Delta S_C^{*} = \Delta H_C^{*} / T_{0C} \tag{12}$$

this leads to:

$$\frac{\Delta H_C^{*}}{R}\left(\frac{1}{T_{0C}} - \frac{1}{T}\right) = m\,ln(1-X) + n\,lnX + \mu^E \tag{13}$$

When $X = \frac{n}{m+n}$, $T = T_{0C}$,

$$\mu^E = -m\ ln\left(\frac{m}{m+n}\right) - n\ ln\left(\frac{n}{m+n}\right)$$

and at the point when $X = \frac{n}{m+n}$

$$\frac{dT}{dX} = 0$$

The phase diagram of MeNQ/AN as reported in a patent [1] is shown in Figure 3. This phase diagram has two eutectic points. Equation (13) is suitable for the MeNQ/AN binary system. Ordinary data on the mole fractions of MeNQ and temperatures corresponding to the phase diagram were obtained and substituted into Equation (13) to construct the binary phase diagram of MeNQ/AN, as shown in Figure 4. Figure 4 demonstrates that important points, such as the eutectic points and the co-crystal point, are very close to those illustrated in Figure 3. This result proves that the equation of the phase diagram with two eutectic points is correct.

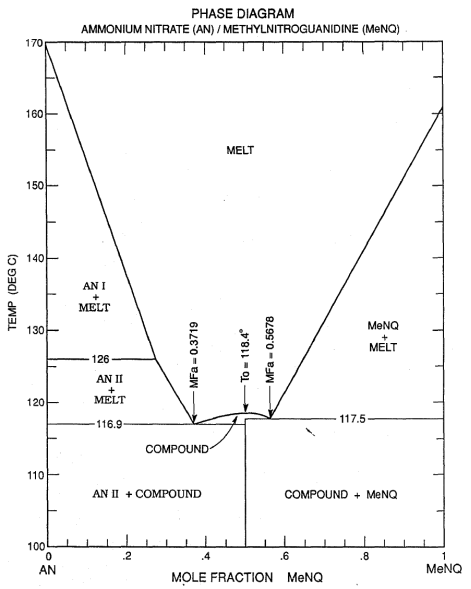

Figure 3. T-X phase diagram of the MeNQ/AN binary system reported in the literature [1].

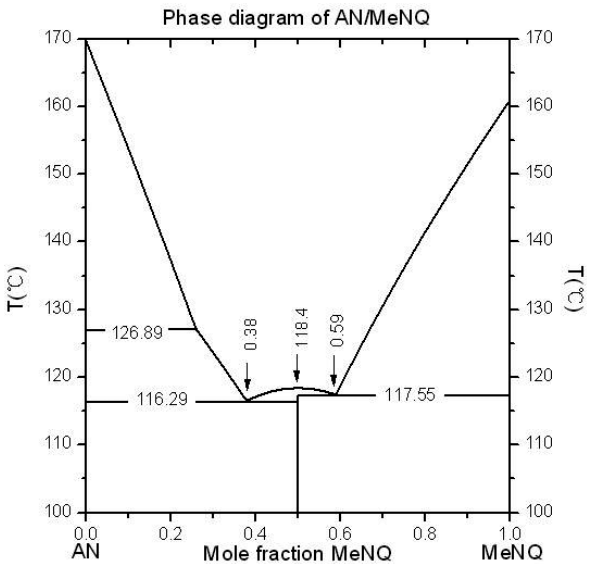

Figure 4. T-X phase diagram of the MeNQ/AN binary system obtained by the equation in this work.

4 Results and Discussion

4.1 DSC curves of the MeNQ/HN and HN/NQ binary systems

The DSC curves of the HN/NQ and MeNQ/HN systems are shown in Figures 5 and 6, respectively. The compositions and melting temperatures of the two systems obtained from the DSC curves are shown in Table 1. The temperature and composition data in Table 1 show that the HN/NQ system has two eutectic points. In the present system, $m = 3$, $n = 1$, $T_{0C} = 227.483$ °C and $\Delta H_C^* = 18.474$ kJ/mol. The T_{0C} and ΔH_C^* were calculated from the expression of the liquid curve of the phase diagram with two eutectic points (Equation 13). The binary system of MeNQ/HN has only one eutectic point.

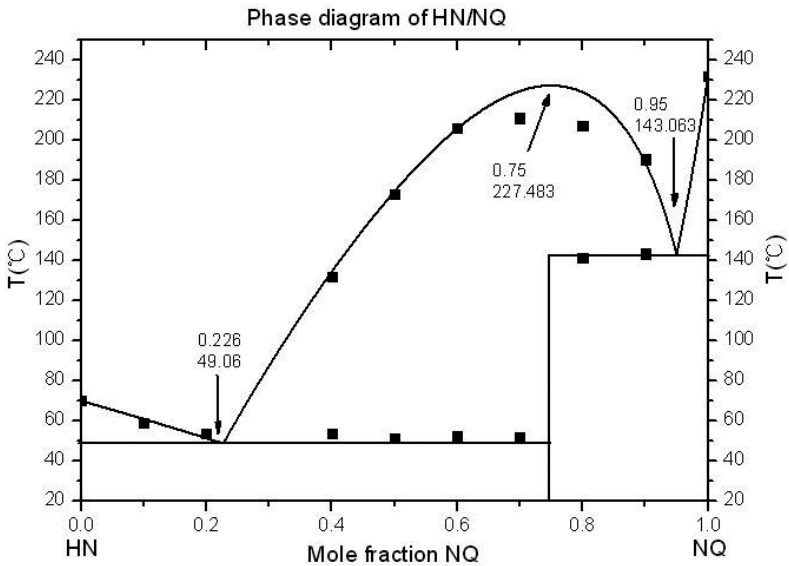

Figure 5. DSC curves of HN/NQ binary systems.

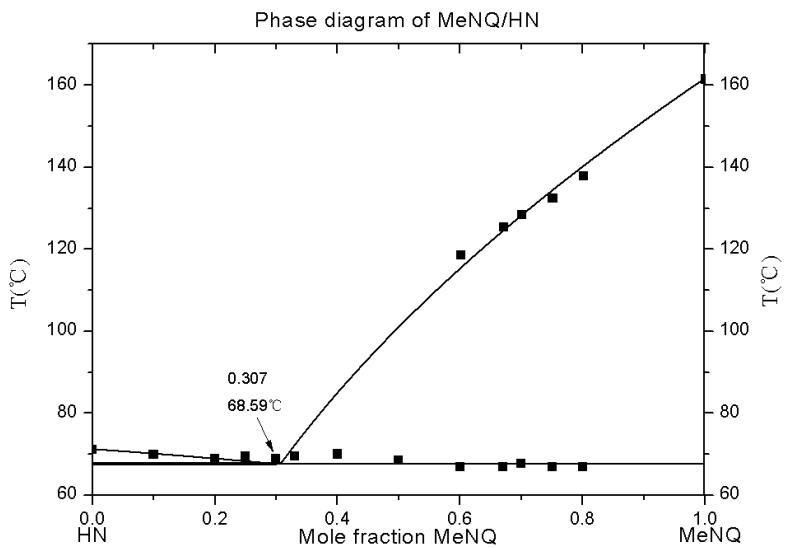

Figure 6. DSC curves of MeNQ/HN binary systems [10].

The DSC curves of HN/NQ are shown in Figure 5. The curve of pure HN is labelled 1, and the mole fraction of NQ in curve 10 is 0.9. The mole fraction of NQ increases from curve 1 to curve 10. In curves 1 to 8, the eutectic melting

peak is approximately 50 °C, and the other peak moves to higher temperatures with increasing NQ content. In curves 9 and 10, the eutectic temperature is near 140 °C. As the system has two eutectic temperatures, it has two eutectic points. The mole fraction of NQ at the co-crystal point is between 0.7 and 0.8.

The prominent peaks for the MeNQ/HN system are shown in Figure 6. Peak 1 appears at temperatures slightly lower than 70 °C, with a second peak (peak 2) appearing when the mole fraction of MeNQ is greater than 0.3 (curves 9, 4, 5, 6, 11, 7, 12, and 8). This peak moves toward higher temperatures with increasing mole fraction of MeNQ. Peak 1 is the melting peak of the eutectic, and peak 2 indicates the melting temperature of MeNQ in the MeNQ/HN binary system.

4.2 Phase diagram of the binary systems

The binary phase diagram of the HN/NQ system was constructed using the method described earlier by substituting m, n, T_{0C}, ΔH_C^* and the data shown in Table 1 into Equation (13). The binary phase diagram of HN/NQ is shown in Figure 7.

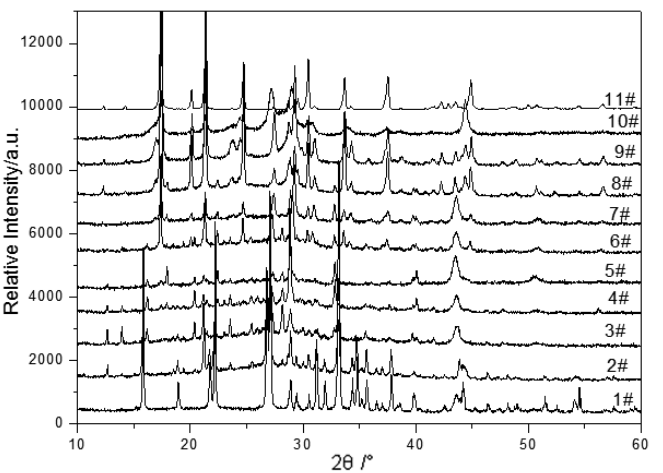

Figure 7. Phase diagram of the HN/NQ binary systems.

This phase diagram has two eutectic points, $X_{NQ} = 0.226$, $T = 49.06$ °C and $X_{NQ} = 0.95$, $T = 143.063$ °C, as marked on the diagram. The point $X_{NQ} = 0.75$, $T = 227.483$ °C is a co-crystal point, a new compound arising at this point. Its enthalpy $\Delta H_C^* = 18.474$ kJ/mol, and its melting point is $T_{0C} = 227.483$ °C, at a mole ratio of HN : NQ = 1 : 3.

There is a single phase area of the liquid mixture of HN and NQ on the liquid curve. The area between the liquid curve and the solid curve is the binary phase area. When $0<X_{NQ}<0.226$, the system contains the liquid phase and HN in the solid state; the solid and liquid coexist when $0.226<X_{NQ}<0.95$. For $0.95<X_{NQ}<1$ there is an area of liquid and solid NQ. Under the solid curves, $0<X_{NQ}<0.75$ is a binary phase area containing HN and the new compound in the solid state, and when $0.75<X_{NQ}<1$, the solid NQ and the new compound coexist.

When $0<X_{NQ}<0.226$, the HN and NQ liquid mixture and HN in the solid state reach equilibrium. The thermodynamic potential of liquid HN should be equal to that of solid HN on any point on the liquid curve ($0<X_{NQ}<0.226$). When $0.226<X_{NQ}<0.95$, the system on the liquid curve is a chemical equilibrium between the liquid mixture and the new compound in the solid state (given in Equation (10)). The liquid curve in the region $0<X_{NQ}<0.226$ describes a solid-liquid equilibrium between solid NQ and the liquid mixture.

As the samples are heated liquify they become yellow, which may be the colour of the new compound. The new substance may be a co-crystal of HN and NQ; this co-crystal exerts a negative effect on the hygroscopicity of the system [31].

The MeNQ/HN system has only one eutectic point. The phase diagram of this system can be constructed using the following equations:

For the left part, $$\ln(1-X)=\frac{\Delta H^{*}_{HN}}{R}\left(\frac{1}{T_{0HN}}-\frac{1}{T}\right)$$

For the right part, $$\ln(X)=\frac{\Delta H^{*}_{MeNQ}}{R}\left(\frac{1}{T_{0MeNQ}}-\frac{1}{T}\right)$$

where X is the mole fraction of MeNQ, ΔH_{HN}^{*} and ΔH_{MeNQ}^{*} are the enthalpies of melting of the pure components HN and MeNQ, respectively, and T_{0HN} T_{0MeNQ} are the melting points of the pure components HN and MeNQ.

The binary phase diagram of the MeNQ/HN system can be constructed using the compositions and temperatures in Table 1, and is shown in Figure 8.

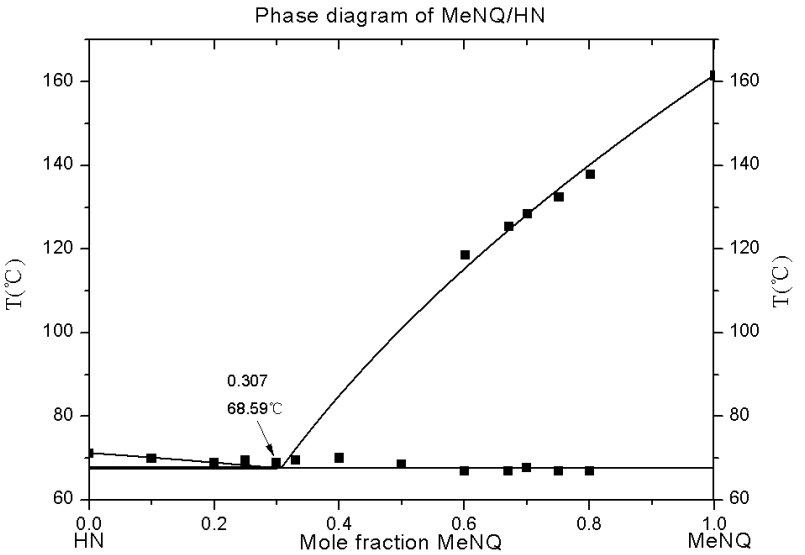

Figure 8. Phase diagram of MeNQ/HN binary systems.

At the eutectic point of the phase diagram shown in Figure 8, the eutectic composition is 0.307 (mole fraction of MeNQ) and the eutectic temperature is 68.59 °C. The eutectic point has three phases: liquid mixture, solid HN and solid MeNQ. The equilibrium in this phase diagram is similar to the solid-liquid equilibrium in the phase diagram of HN/NQ. No new substance was produced at any ratio in this system.

4.3 XRD patterns of the samples

The crystal structures of the eutectic mixtures were studied by XRD. The XRD patterns of HN/NQ and MeNQ/HN are shown in Figures 9 and 10, respectively.

In Figure 9, curve 1 is the XRD pattern of pure HN, curve 11 is the XRD pattern of pure NQ, and curves 2-10 are the XRD patterns of the eutectic mixture. Compared with the XRD pattern of the pure components, new peaks appear at $2\theta = 12.67$, 16.20, 17.93, 20.43, 28.18, 32.84, and 40.09° in the XRD patterns of the eutectic mixture. Thus, there may be new crystals growing in the mixture of HN and NQ. A similar result has been previously reported [19].

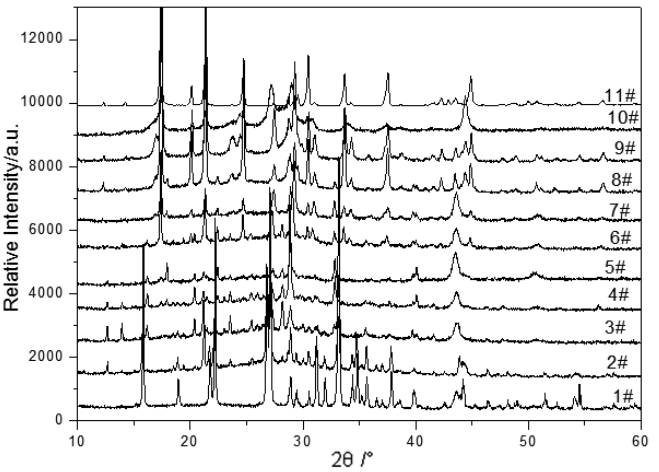

Figure 9. XRD pattern of HN/NQ binary systems.

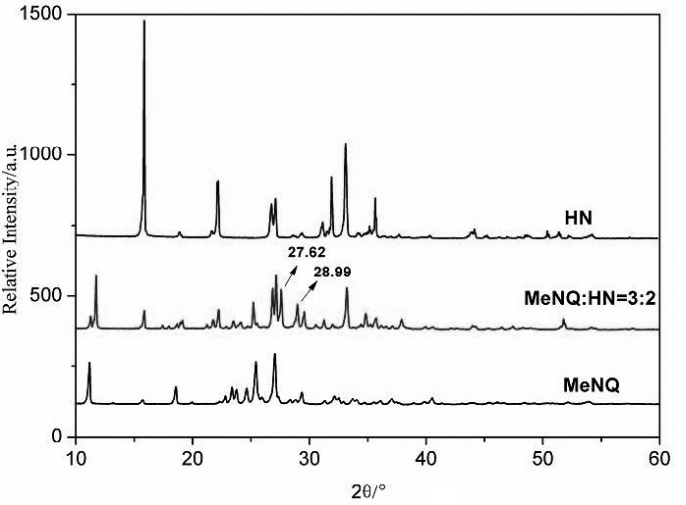

Figure 10. XRD pattern of MeNQ/HN binary systems [10].

The XRD patterns in Figure 10 show patterns for the mixture, pure HN, and MeNQ. These patterns were considered to be new peaks and thus new crystals at 2θ = 27.62 and 28.99° in a previous paper [10]. Further analysis of the experimental data shows that the two peaks marked in Figure 9 at 2θ = 27.5889 and 28.9783°, and not at 2θ = 27.62 and 28.99°, correspond to the peaks 2θ = 27.3422 and 28.8459° in the pattern of MeNQ. The slight variations

in angles are acceptable. Therefore, no new peaks and no new crystals are generated, in agreement with the above phase diagram result.

5 Conclusions

The expressions for binary phase diagrams with one eutectic point and two eutectic points were deduced on the basis of phase equilibrium theory. The binary phase diagram of HN/NQ was constructed using the corresponding equation and the experimental data. Thus, a new method for constructing phase diagrams with two eutectic points, without the need to gather large amounts of experimental data, was demonstrated. We deduced from the binary phase diagram of HN/NQ that a new compound is generated during the uniform mixing of HN and NQ on heating. The new compound may be a co-crystal of these two components. The XRD patterns verified this deduction.

A phase diagram of the MeNQ/HN binary system with only one eutectic point was constructed by substituting the experimental results (reported in article [11]) into Equation (9) (Van't Hoff equation). A eutectic mixture was produced, but no new substance was generated. The XRD patterns verified this.

The structure and properties of the compound obtained in the HN/NQ system, as well as the eutectic obtained in the MeNQ/HN system, will be the focus of further work.

Acknowledgments

The authors are grateful for financial support from the National Natural Science Foundation of China – CAEP project (No. 11076002).

6 References

[1] Patrick M.A., Aubert S.A., *Intermolecular Complex Explosives*, US Patent 4 948 438, **1990**.

[2] Zhang G.-Q., Dong H.-S., Synthesis Progress and Application of N-Methyl-N'-nitroguanidine in Melt/Cast Explosives (in Chinese), *Chin. J. Energ. Mater.*, **2008**, *16*(3), 353-355.

[3] Chen L., Shu Y.-J., Xu R.-J., Xu T., Wang X.-F., Review on Energetic Eutectic (in Chinese), *Chin. J. Energ. Mater.*, **2013**, *21*(1), 108-115.

[4] Bonn O., Hammerl A., Klapötke T.M., Mayer P., Piotrowski H., Zewen H., Plume Deposits from Bipropellant Rocket Engines: Methylhydrazinium Nitrate and N,N-Dimethylhydrazinium Nitrate (in German), *Zeitschrift für anorganische*

undallgemeine Chemie, **2001**, *627*(8), 2011-2015.
[5] Shu Y.-J., Huo J.-C., *Introduction to Explosive* (in Chinese), Chemical Industry Press, Beijing, **2011**, p. 162.
[6] Shu Y.-J., Li H.-R., Xiong Y., Zhou Y., Qian W., Some Problems in Theoretical Design of Energetic Materials, *Chin. J. Energ. Mater.*, **2013**, *21*(2), 166-172.
[7] Hariharanath B., Chandrabhanu K.S., Rajendran A.G., Ravindran M., Kartha C.B., Detonator Using Nickel Hydrazine Nitrate as Primary Explosive, *Def. Sci. J. − New Delhi*, **2006**, *56*(3), 383.
[8] Zarko V.E., Simonenko V.N., Anisiforov G.I., Aparin A.V., Combustion Characterization of Hydrazinium Nitrate/Energetic Binder/Alex Based Model Propellants, *Aerosp. Sci. Technol.*, **2007**, *11*(1), 13-17.
[9] Klapötke T.M., Rienäcker C.M., Zewen H., Calculated and Experimentally Obtained Heats of Combustion of Hydrazinium Nitrate, Monomethyl Hydrazinium Nitrate and N, N-Dimethyl Hydrazinium Nitrate (in German), *Zeitschrift für anorganische und allgemeine Chemie*, **2002**, *628* (11), 2372-2374.
[10] Chen L., Li H.-R., Xiong Y., Xu R.-J., Xu T., Liu X.-F., Shu Y.-J., Structure and Molecular Interaction of Methyl-nitroguanidine and Hydrazine Nitrate Eutectics (in Chinese), *Chin. J. Energ. Mater.*, **2012**, *20*(5), 560-564.
[11] Venault L., Moisy P., Blanc P., Madic C., Kinetics of Hydrazinium Nitrate Decomposition in Nitric Acid Solutions under the Effect of Power Ultrasound, *Ultrason. Sonochem*., **2001**, *8*(4), 359-366.
[12] Croker D.M., Foreman M.E., Hogan B.N., Maguire N.M., Elcoate C.J., Hodnett B.K., Maguire A.R., Rasmuson Å.C., Lawrence S.E., Understanding the p-Toluenesulfonamide/Triphenyl Phosphine Oxide Crystal Chemistry: a New 1:1 Cocrystal and Ternary Phase Diagram, *Cryst. Growth Des.*, **2011**, *12*(2), 869-875.
[13] Feigenson G.W., Buboltz J.T., Ternary Phase Diagram of Dipalmitoyl-PC/Dilauroyl-PC/Cholesterol: Nanoscopic Domain Formation Driven by Cholesterol, *Biophys. J.*, **2001**, *80*(6), 2775-2788.
[14] Good D.J., *Pharmaceutical Cocrystal Eutectic Analysis: Study of Thermodynamic Stability, Solubility, and Phase Behavior*, The University of Michigan, **2010**.
[15] Ren Z.-A., Che G.-C., Dong X.-L., Yang J., Lu W., Yi W., Shen X.-L., Li Z.-C., Sun L.-L., Zhou F.-R., Superconductivity and Phase Diagram in Iron-based Arsenic-oxides $ReFeAsO_{1-\delta}$ (Re= Rare-earth Metal) without Fluorine Doping, *Europhys. Lett*., **2008**, *83*(1), 17002.
[16] Schiffer P., Ramirez A.P., Bao W., Cheong S.W., Low Temperature Magnetoresistance and the Magnetic Phase Diagram of $La_{1-x}Ca_xMnO_3$, *Phys. Rev. Lett*., **1995**, *75*(18), 3336.
[17] Shao Y.-H., Ren X.-N., Liu Z.-R., Zhang X., Ternary Phase Diagrams of DNTF and TNAZ and Their Eutectics, *J. Therm. Anal. Calorim.*, **2011**, *103*(2), 617-623.
[18] Liu Y., Liu Z.-R., Yin C.-M., The Phase Diagram and Eutectic of Binary Systems for 1, 3, 3-Trinitroazetidine (TNAZ) with Some Energetic Materials (in Chinese), *Chin. J. Energ. Mater.*, **2004**, 227-230.
[19] Chen L., Li H.-R., Xu R.-J., Xiong Y., Xu T., Huang B.-Y., Shu Y.-J., Solidification

Behavior of the Hydrazine Nitrate-Nitroguanidine Eutectic System, *Propellants Explos. Pyrotech.*, **2013**, *39*(2), 217-223.

[20] Foo M. L., Wang Y. Y., Watauchi S., Zandbergen H.W., He T., Cava R.J., Ong N.P, Charge Ordering, Commensurability, and Metallicity in the Phase Diagram of the Layered Na_xCoO_2, *Phys. Rev. Lett.*, **2004**, *92*(24), 247001.

[21] Ren X.-N., Heng S.-Y., Shao Y.-H., Liu Z.-R., Zhang X., Wang X.-H., Han F., The Binary Phase Diagram and Eutectic System for DNTF/PETN (in Chinese), *Chin. J. Energ. Mater.,* **2009**, *17*(4), 455-458.

[22] Witusiewicz V.T., Sturz L., Hecht U., Rex S., Phase Equilibria and Eutectic Growth in Quaternary Organic Alloys Amino-methyl-propanediol-(D) Camphor-Neopentylglycol-Succinonitrile (AMPD-DC- NPG-SCN), *J. Cryst. Growth*, **2006**, *297*(1), 117-132.

[23] Witusiewicz V.T., Hecht U., Sturz L., Rex S., Phase Equilibria and Eutectic Growth in Ternary Organic System (D)camphor-neopentylglycol-succinonitrile, *J. Cryst. Growth*, **2006**, *286*(2), 431-439.

[24] Witusiewicz V.T., Hecht U., Sturz L., Rex S., Phase Equilibria and Eutectic Growth in Ternary Organic System Amino-methyl-propanediol-(D)camphor-neopentylglycol, *J. Cryst. Growth*, **2006**, *286*(1), 137-145.

[25] Liu Z.-R., Shao Y.-H., Yin C.-M., Kong Y.-H., Measurement of the Eutectic Composition and Temperature of Energetic Materials. Part 1. The Phase Diagram of Binary Systems, *Thermochim. Acta*, **1995**, *250*(1), 65-76.

[26] Yin C.-M., Liu Z.-R., Shao Y.-H., Kong Y.-H., Measurement of the Eutectic Composition and Temperature of Energetic Materials. Part 2. The HX-phase Diagram of Ternary Systems, *Thermochim. Acta*, **1995**, *250*(1), 77-83.

[27] Kong Y.-H., Liu Z.-R., Shao Y.-H., Yin C.-M., He W., Measurement of the Eutectic Composition and Temperature of Energetic Materials. Part 3. The TX-phase Diagram of Ternary System, *Thermochim. Acta*, **1997**, *297*(1), 161-168.

[28] Chapman R.D., Fronabarger J.W., A Convenient Correlation for Prediction of Binary Eutectics Involving Organic Explosives, *Propellants Explos. Pyrotech.*, **1998**, *23*, 50-55.

[29] Reich L., Melting and Decomposition of RDX-HNX Mixtures by DTA, *Thermochim. Acta*, **1973**, *7*, 57-67.

[30] Reisman A., *Phase Equilibria*, Academic Press, New York , p. 130.

[31] Trask A.V., Samuel W.D.M., William J., Pharmaceutical Co-crystallization: Engineering a Remedy for Caffeine Hydration, *Cryst. Growth. Des.*, **2005**, *5*(3), 1013-1021.